

Molecular modelling of Me^{2+} - (8-hydroxy-quinolate)₂ complexes using ZINDO and ESSF methods

Dan V. Nicolau and Susumu Yoshikawa

Osaka National Research Institute, Osaka, Japan

The Me^{2+} (8-hydroxyquinolate)₁₋₂ system was studied using semi-empirical (ZINDO) and molecular mechanics (ESSF) methods for a range of bivalent metals comprising alkaline earth metals (up to Sr^{2+}) and the first two rows of transition metals. The structural validation of the optimisation calculations showed that ESSF is in general an efficient predictor of the structure of the complexes. On the other hand, ZINDO offers an appropriate tool for describing the mechanisms of complex formation for the studied system. The spectral validation based on the comparison of spectral data with predicted molecular geometric parameters shows that ZINDO offers a better tool for describing the mechanisms of complex formation. Finally, the consistent relationship (in relative terms) between SCF energies and equilibrium constants, and between computed charges at the oxygen ligation atom and pH, showed that ZINDO can be used as a tool for the design of chelating agents. For the system studied the CPU times are not prohibitive, even for a metal-comprehensive investigation. © 1998 by Elsevier Science Inc.

INTRODUCTION

The formation of metal–organic ligand complexes is important to many processes, ranging from the formation of protein supramolecular assemblies to technological processes, for example, solvent extraction and environmental remediation. This importance of the metal–organic ligand system found expression in classical literature,¹ and in comprehensive databases comprising experimentally resolved molecular structure of metal–organic ligand complexes (e.g., see Ref. 2). Still, many questions regarding the more complex, but not less important, interaction of the atomic orbitals inside the molecular complex and the interaction of the molecule complex with its surround-

ing environment have proven more difficult to answer. This difficulty arises, especially in the case of complexes of transition metals, from the interaction of metallic orbitals (e.g., *d* orbitals) with the orbitals of the organic ligand (e.g., π orbitals). It follows that molecular modelling is a natural complement to experimental studies.

To validate the seamless applicability of present molecular modelling tools and techniques to the accurate description of the metal–organic ligand complexes a study should choose (1) techniques that cover a large range of metals, (2) systems that are experimentally well described in the literature to allow a thorough validation, (3) wherever possible, systems that have widespread applicability, and (4) by preference, techniques that are not prohibitive in terms of computer resources. The first and the last requirements from the preceding list were met in the present study through the use of a classic semi-empirical approach (i.e., ZINDO³) and a rather novel molecular mechanics approach (ESSF⁴). *Ab initio* studies, although thorough and comprehensive,⁵ would impose a relative high penalty in terms of computer resources for similar metal-comprehensive studies. Other metal-comprehensive methods, that is, PM3tm⁶ and MOME⁷, were in their initial stages when the present study started. The second and third requirements in the preceding list were met by the choice of the Me^{2+} (8-hydroxyquinolate)₁₋₂ system, which is relevant to a wide range of applications (e.g., analytical chemistry,⁸ solvent extraction,⁹ and ion-exchange processes¹⁰), and therefore it was studied extensively with experimental techniques.¹¹

METHODS

Computational chemistry approaches

Two computational chemistry approaches have been used: (1) a molecular mechanics approach, that is, ESSF (Extensive Systematic Force Field), as implemented in the Discover 3 module of Molecular Simulations, Inc. (MSI) software,¹² and (2) a semi-empirical approach, that is, ZINDO, as implemented in the ZINDO module of MSI software.¹³

ESSF allows the study of complexes with most bivalent ions taken into consideration in this study (i.e., alkaline earth metals

Color Plates for this article are on pages 99–100.


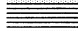






Address reprint requests to: Dan V. Nicolau, Rio Tinto/Research and Technology Development, Locked Bag 347, Bentley Delivery Centre, Perth, WA 6983, Australia. e-mail: Dan.Nicolau@riotinto.com.au.

Table 1. Coverage of Studied Bivalent Metals by ESFE and ZINDO Methods



		ESFF potential type																ZINDO's Gammas			
At.no.	Me ²⁺	022	022t	023	024	024l	024s	024t	025	025s	025t	026	026o	027l	027p	028h	02d	theoretical	spectroscopical	Me ²⁺	At.no.
4	Be																			Be	4
12	Mg																			Mg	12
20	Ca																			Ca	20
21	Sc																			Sc	21
22	Ti																			Ti	22
23	V																			V	23
24	Cr																			Cr	24
25	Mn																			Mn	25
26	Fe																			Fe	26
27	Co																			Co	27
28	Ni																			Ni	28
29	Cu																			Cu	29
30	Zn																			Zn	30
38	Sr																			Sr	38
39	Y																			Y	39
40	Zr																			Zr	40
41	Nb																			Nb	41
42	Mo																			Mo	42
43	Tc																			Tc	43
44	Ru																			Ru	44
45	Rh																			Rh	45
46	Pd																			Pd	46
47	Ag																			Ag	47
48	Cd																			Cd	48

LEGEND: Availability of parametrisation

ESFF potential type

-  = bi_coordination
-  = tri_coordination
-  = tetra_coordination (preferred)
-  = penta_coordination
-  = hexa_coordination
-  = hepta_coordination
-  = octahedral_coordination
-  = linear_coordination

ZINDO

-  = theoretical gamma (used for optimisation)
-  = spectroscopical gamma (used for energy estimation)

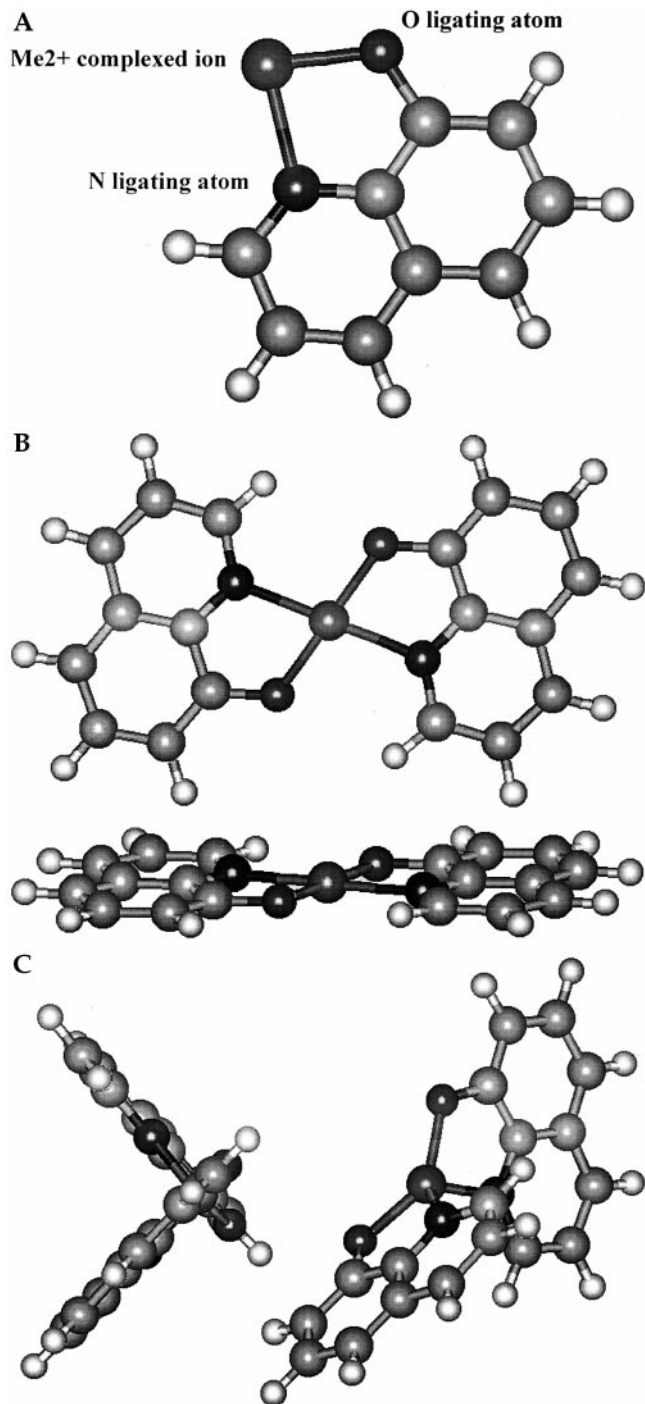


Figure 1. Model structures of monodentate and bidentate $\text{Me}^{2+}(\text{8-hydroxyquinolate})_{1-2}$ complexes. (A) Monodentate $\text{Me}^{2+}(\text{8-hydroxyquinolate})$ complex; (B) bidentate square-planar $\text{Me}^{2+}(\text{8-hydroxyquinolate})_2$ complex; (C) bidentate tetrahedral $\text{Me}^{2+}(\text{8-hydroxyquinolate})_2$ complex.

and the first two rows of transition metals) except scandium and yttrium. ESFF is a “rule-based” force field, that is, the user must specify the oxidation state and the coordination type of the respective atom. The 2+ oxidation state covered for the metallic ions in this study with their coordination is presented

in Table 1. The denomination of ESFF options points to (1) the oxidation state of the metallic ion (2+; the first two digits, i.e., 02), (2) coordination number (2 through 8, and 1 for linear; the third digit/symbol), (3) coordination type (l, s, t, p, o, h, d, for C_{2v} , D_{4h} , T_d , O_h , D_{5h} , $\text{D}_{2h}/\text{D}_{3h}$, D_{∞} symmetry type, respectively; the fourth symbol—optional).

ZINDO allows the study of complexes of all bivalent ions taken into consideration in this study, except strontium. The elements covered by ZINDO as implemented in MSI software are also presented in Table 1. ZINDO is not designed to be used for robust optimisation.^{13,14} Hence careful procedures should be used for reaching reasonable structures during optimisation, especially when nonplanar structures are sought.

A third approach, that is, *ab initio* as implemented in the DMol module of MSI software,¹⁵ has been used for a limited number of bidentate complexes (planar complexes from manganese throughout to zinc, and nonplanar complexes for copper and zinc).

Computational procedures

The complexes studied comprised the molecular structures with the general formula MeL_i , where Me is a bivalent metal ion in the second principal group up to Sr^{2+} or in the first or second row of transition metals, L is the chelating ligand, that is, 8-hydroxyquinoline, and *i* equals 1 for monodentate complexes and 2 for bidentate complexes. The data associated with the molecular models comprised (1) structural data (geometry of the centre, bond lengths and angles), (2) energy data (energies associated with the structures, i.e., bonded/unbonded energies from molecular mechanics calculations, electronic energies from semi-empirical calculations), and (3) partial charges localised at atoms.

The structures were firstly optimised using the ESFF molecular mechanics force field, using all force fields associated with ESFF (as in Table 1). It is reasonable to assume that appropriate results can be obtained only by using the ESFF 2-coordination option (i.e., 022 or 022t) for monodentate complexes and the 4-coordination option (i.e., 024, 024l, 024s, and 024t) for bidentate complexes. However, to assure the comprehensiveness of the calculations, the structures were optimised using all ESFF options available, but the further processing of the data used mainly 2- and 4-coordination options. The optimisation process proceeded until a 0.001 gradient (in atomic units) was reached. The parameters of the ESFF optimised structures were further used in the study.

The structures optimised with ESFF that were the closest to the square-planar and tetrahedral geometry were submitted to ZINDO optimisation (with theoretical γ values). The optimisation progressed smoothly for planar structures irrespective of the method used (ESFF or ZINDO). However, ZINDO optimisation of nonplanar structures required a stepwise optimisation approach: (1) start with tetrahedral geometries predicted by ESFF; (2) optimise in steps, advancing from lower gradients (around 0.01 a.u.) towards more optimised structure; (3) stop the stepwise optimisation when the structures begin to distort heavily; (4) discard heavily distorted structures and retain the last optimisation for further analysis. The difficulties encountered in the optimisation of nonplanar structures were somehow anticipated owing to the expected influence of the Jahn–Teller effect in transition metal complexes. The symmetry was maintained during all

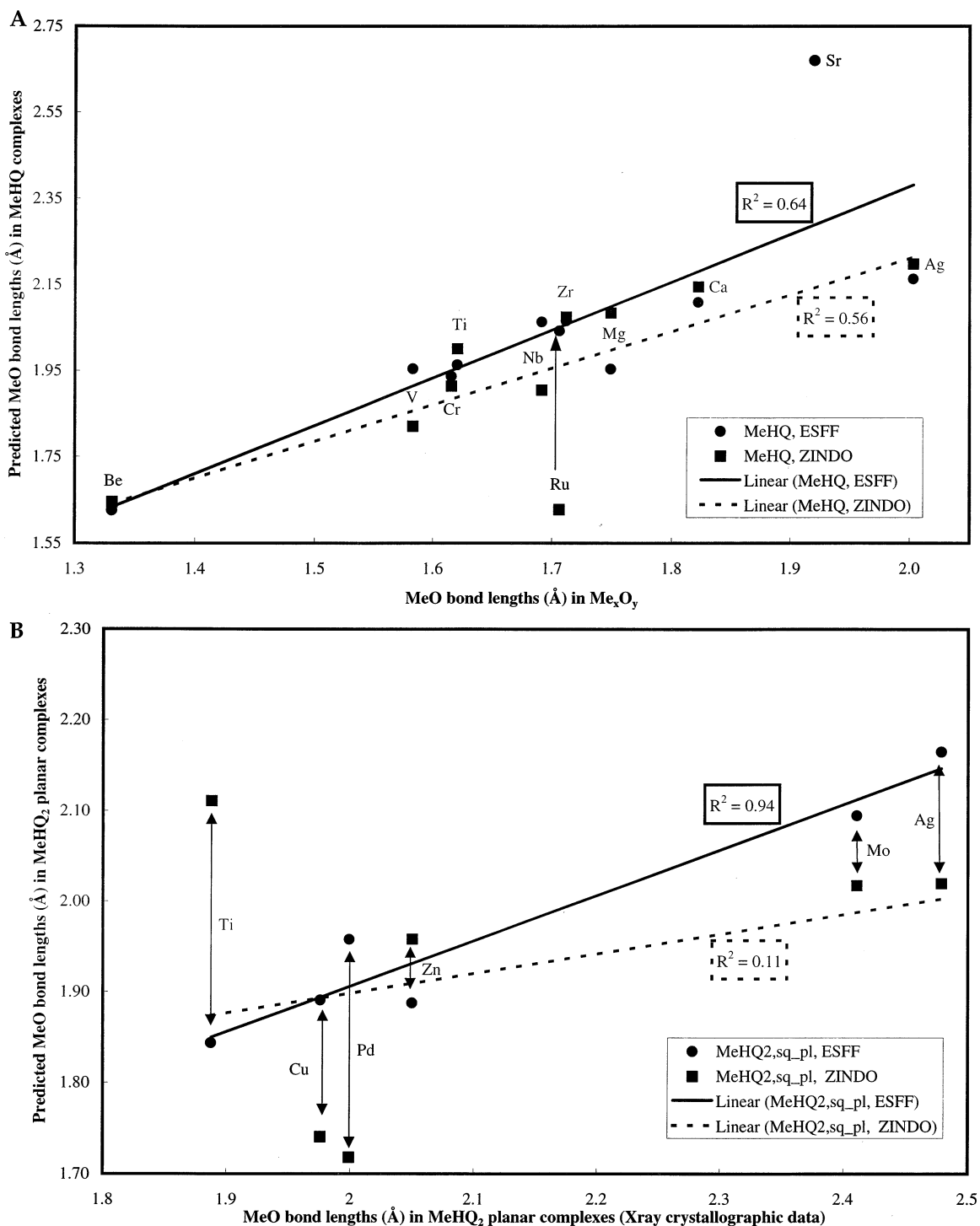


Figure 2. Experimental versus predicted bond lengths for the structures optimised with ESFF and ZINDO. (A) MeO bond lengths in Me_xO_y (experimental values, gas phase) versus the MeO bond lengths in monodentate MeHQ complexes (predicted); (B) MeO bond lengths in square-planar MeHQ₂ complexes (X-ray crystallographic data) versus MeO bond lengths in square-planar MeHQ₂ complexes (predicted); (C) MeN bond lengths in square-planar MeHQ₂ complexes (X-ray crystallographic data) versus MeN bond lengths in square-planar MeHQ₂ complexes (predicted).

optimisations. In the case of planar structures the optimisation proceeded until a 0.001 gradient was reached, but for nonplanar structures the gradient that could be achieved varied from 0.01 to 0.003. The square-planar (either perfect

or distorted) and tetrahedral structures, except those of silver and cadmium complexes, were further submitted to ZINDO energy calculations with spectroscopic γ values.¹³ The parameters of the structures optimised with ZINDO with the-

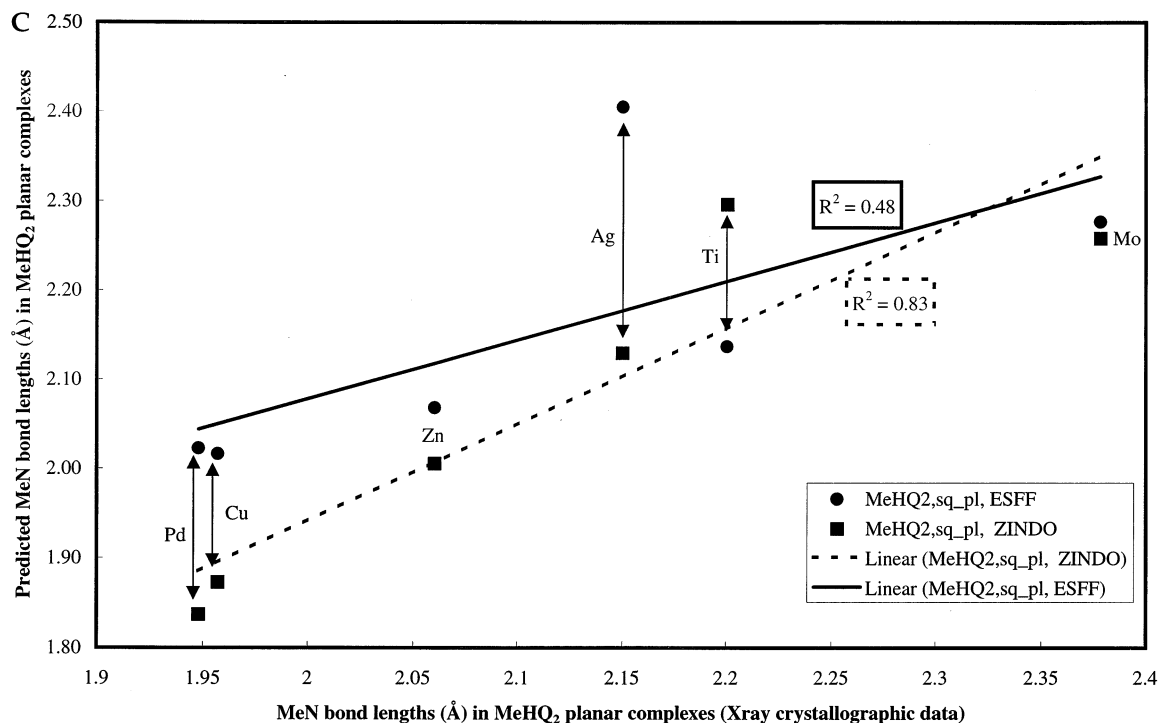


Figure 2. Continued.

oretical γ values and from energy calculations with ZINDO with spectroscopic γ values were further used in the study.

Ab initio calculations used the ZINDO-optimised structures as the starting point of optimisation, but because of computer resource constraints the optimisation did not progress up to fully optimised structures.

RESULTS

Planar versus nonplanar structures

All monodentate complexes (the first step in the formation of complexes with superior coordination) presented planar structures, irrespective of the options used with ESFF or ZINDO (as in Figure 1A). Bidentate complexes presented two major classes of structures, namely square-planar structures (as in Figure 1B) or tetrahedral structures (as in Figure 1C). These classes also contain some slightly distorted structures. In some isolated cases (e.g., calcium) a third pyramidal class could be found and only for ESFF optimisations. The 027p ESFF potential type also produced pyramidal structures. This third class was not further analysed thoroughly owing to the higher coordination, or because of their singularity.

Structural validation of the optimised structures

The structural validation of the optimised structures progressed on two lines, that is: (1) validation based on the comparison of the predicted bond lengths with experimental values; and (2) validation based on the overall comparison of the structures computed with experimentally proven structures or, when these were not available, with the structures predicted by high-level *ab initio* computations.

The structural validation based on the bond lengths com-

prised the comparison of (1) predicted MeO bond lengths with respect to MeO bond lengths in the corresponding metal oxides in the gas phase¹⁶ (Figure 2A), and (2) predicted MeO bond lengths (Figure 2B) and (3) predicted MeN bond lengths (Figure 2C) with respect to bond lengths in corresponding structures, as reported in the Cambridge Crystallographic Data Base.^{17–24}

The structural validation based on the RMS overlay of structures comprised the comparison of (1) the predicted square-planar $\text{Cu}^{2+}(\text{8-hydroxyquinolate})_2$ structure optimised with ZINDO with those reported in Ref. 18 (Figure 3A; α , β , and γ forms); (2) the predicted planar $\text{Zn}^{2+}(\text{8-hydroxyquinolate})_2$ structure optimised with ZINDO with the structure reported in Ref. 19 (Figure 3B; octahedral structure in dihydrate form with water molecules removed); (3) the predicted square-planar $\text{Cu}^{2+}(\text{8-hydroxyquinolate})_2$ structures (Figure 3C; for ZINDO, ESFF Cu024s, ESFF Cu024l, and DMol); (4) the predicted square-planar $\text{Zn}^{2+}(\text{8-hydroxyquinolate})_2$ structures (Figure 3D; for ZINDO, ESFF Zn024, and DMol); (5) the predicted tetrahedral $\text{Cu}^{2+}(\text{8-hydroxyquinolate})_2$ structures (Figure 3E; ZINDO, ESFF Cu024t, and DMol); and (6) the predicted tetrahedral $\text{Zn}^{2+}(\text{8-hydroxyquinolate})_2$ structures (Figure 3F; ZINDO, ESFF Zn024, and DMol).

DISCUSSION

$\text{Me}^{2+}(\text{8-hydroxyquinolate})_{1-2}$ complexes

The choice of the molecular system to be studied with molecular modelling using a *single-molecule approach* should be governed, in addition to the considerations outlined in the introductory section, by the high degree of independence be-

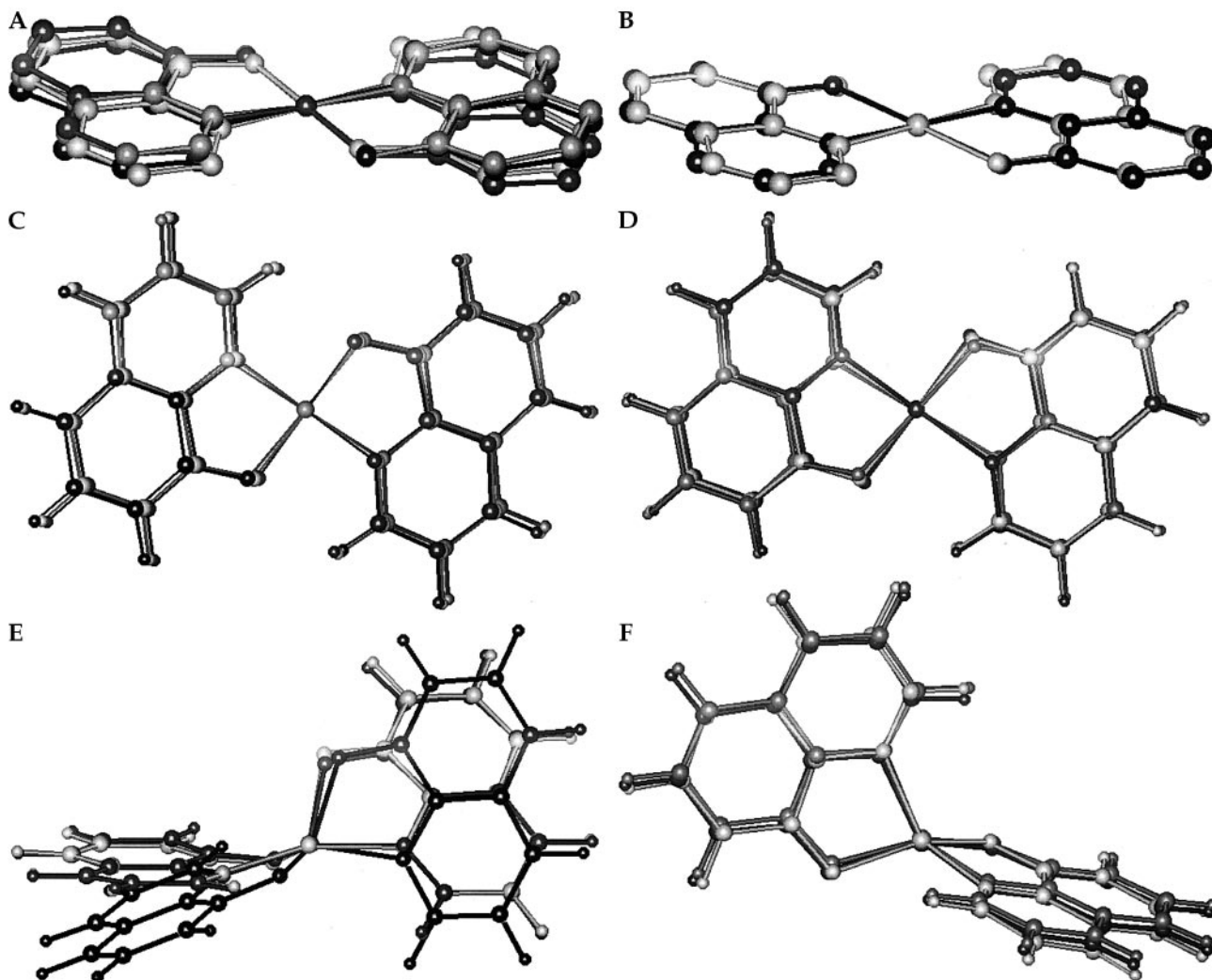


Figure 3. RMS overlay of the computed and experimental or ab initio $\text{Me}^{2+}(\text{8-hydroxyquinolate})_2$. (A) Planar $\text{Cu}^{2+}(\text{HQ})_2$ structure optimised with ZINDO (lightest grey) versus X-ray crystallographic structures (α form, black; β form, medium grey; γ form, darkest grey); (B) $\text{Zn}^{2+}(\text{HQ})_2$ structure optimised with ZINDO (grey) versus dihydrate form with the water molecules removed (black); (C) planar $\text{Cu}^{2+}(\text{HQ})_2$ structures optimised by different methods (ZINDO, darkest grey; ESFF Cu024s, black; ESFF Cu024l, medium grey; DMol, lightest grey); (D) planar $\text{Zn}^{2+}(\text{HQ})_2$ structures optimised by different methods (ZINDO, black; ESFF Zn024, dark grey; DMol, light grey); (E) nonplanar $\text{Cu}^{2+}(\text{HQ})_2$ structures optimised by different methods (ZINDO, dark grey; ESFF Cu024t, black; DMol, light grey); (F) nonplanar $\text{Zn}^{2+}(\text{HQ})_2$ structures optimised by different methods (ZINDO, black; ESFF Zn024, dark grey; DMol, light grey).

tween monomolecular- and multimolecular-driven phenomena. 8-Hydroxyquinoline and its derivatives are extremely insoluble in water. Moreover, the affinity of 8-hydroxyquinoline for a large range of metallic ions is high. As a result, the process of the formation and subsequent transport of the metal-organic complexes is an interface-driven phenomenon, as thoroughly proven by numerous experimental studies.¹¹ A significant concentration of the complexes with coordination higher than 4 (required to neutralise the charges at the extracted metal) is unlikely in the aqueous phase, and therefore supramolecular assemblies are unlikely to form in aqueous phase. Complexes with higher coordination are more probable in the bulk organic phase, where the concentration of the extractant is high, but then the formation of supramolecular complexes will be a post-solvent extraction process at the molecular level.

Among the extractants used for analytic solvent extraction, 8-hydroxyquinoline is one of the most versatile (at least 50 metals are known to form complexes with this ligand⁸). Moreover, 8-hydroxyquinoline is the "core" of Kelex 100,²⁴ a powerful extractant used in industrial solvent extraction. Early studies⁸ showed that Be^{2+} , Mg^{2+} , La^{3+} , TiO^{2+} , ZrO^{2+} , Th^{4+} , VO^{2+} , Mn^{2+} , Fe^{3+} , Pd^{2+} , Cu^{2+} , Al^{3+} , Ga^{3+} , In^{3+} , and Pb^{2+} are extracted as chelates of the type MeL_n ; Ca^{2+} , Sc^{2+} , Co^{2+} , UO^{2+} , and Sr^{2+} are extracted as MeL_nHL ; and Ba^{2+} , Zn^{2+} , Cd^{2+} , and Ni^{2+} form extractable complexes of the type $\text{MeL}_n(\text{HL})_2$. Other studies (Cai et al.²⁵ for Ni^{2+} ; Boumezioud et al.²⁶ for Ni^{2+} and Co^{2+} ; Merrit et al.¹⁹ for Zn^{2+}) proved that bivalent metals can generally form bidentate MeL_2 complexes.

Hence, the present study focuses on the molecular modelling of the MeL_2 type of complex to all bivalent ions in the second

principal group (from Be^{2+} to Sr^{2+}) and in the first and second rows of the transition metals. The bivalent metals in the third up to the seventh group (e.g., lead and bismuth) were not included in this study owing to a lack of parametrisation for ZINDO beyond the third principal group and beyond the atoms with [Xe] kernel.

ZINDO versus ESFF approach

Both methods used in this study were chosen for their metal comprehensiveness. This advantage is partially blunted by the specific problems associated with the ZINDO and ESFF approaches. In the context of this study, the major drawbacks of ZINDO are as follows: (1) as outlined previously, ZINDO does not produce automatically robust geometry optimisation,¹⁴ as, for example, PM3; and (2) the SCF energy calculated by ZINDO is not a good predictor of enthalpy *in absolute terms*. In addition to these specific drawbacks, ZINDO cannot be used for molecular dynamics simulations because of its less robust structure prediction and because of prohibitive computer power requirements. Also, in the context of this study, the major drawbacks of ESFF are as follows: (1) ESFF is a “rule-based” force field in which the user must specify the coordination of the metal; (2) because ESFF is a coordination-specific force field it cannot be used for molecular dynamics simulations, as can other molecular mechanics methods.

Further considerations should be accounted for before proceeding to the discussion of the results:

1. ZINDO calculations with spectroscopic γ values offer a better correlation with the properties of the studied complexes than those with theoretical γ values. Hence the latter method was used to obtain the optimised structures and the former to generate data used in analysis.

2. SCF energies for the complexes studied are not directly linked in absolute terms with the enthalpies of formation for the monodentate and bidentate complexes. However, we found that the difference between SCF energies and enthalpy- and enthalpy-associated properties of the respective complexes has a systematic behaviour. Hence, we used SCF energies as an indicator *in relative terms* of the enthalpy- and enthalpy-related parameters.
3. The analysis of ESFF-generated data in terms of energy used only the total potential energy. Important conclusions may be drawn by analysing the other forms of energy reported by ESFF calculations, but this was considered to be beyond the scope of this study. It is, however, the intention of the authors to pursue this line of research in the near future.

With these considerations in mind, the present work attempts to quantify to what extent molecular modelling using the most metal-comprehensive methods can be used in the study of metal-organic ligand complexes in a predictive manner, with $\text{Me}^{2+}(\text{8-hydroxyquinolate})_2$ as the study case.

Molecular modelling studies of $\text{Me}^{2+}(\text{8-hydroxyquinolate})_{1-2}$ complexes

Few studies have used molecular modelling of $\text{Me}^{2+}(\text{8-hydroxyquinolate})_2$ complexes, the most notable being an early exploratory study of solvent extraction complexes,²⁷ a study of Zn^{2+} extraction by substituted 8-hydroxyquinolines in the presence of various pyridinic adducts,²⁸ and more recently a study aiming at molecular design of selective extractants for a wider range of metals.²⁹

However, all these studies were limited by the state of development of the molecular mechanics force fields at that

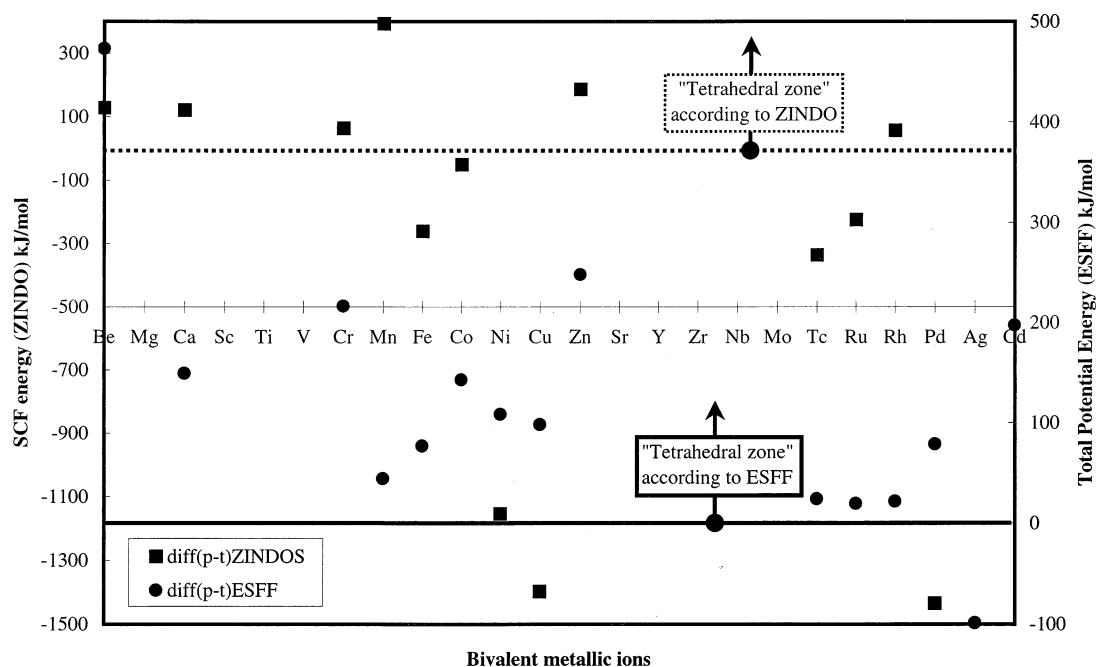


Figure 4. Propensity for the formation of tetrahedral structures versus square-planar structures for bidentate $\text{Me}^{2+}(\text{8-hydroxyquinolate})_2$ complexes, computed with ZINDO (SCF energy) and ESFF (total potential energy). The ordinate axis represents the difference between respective energies of square-planar and tetrahedral complexes.

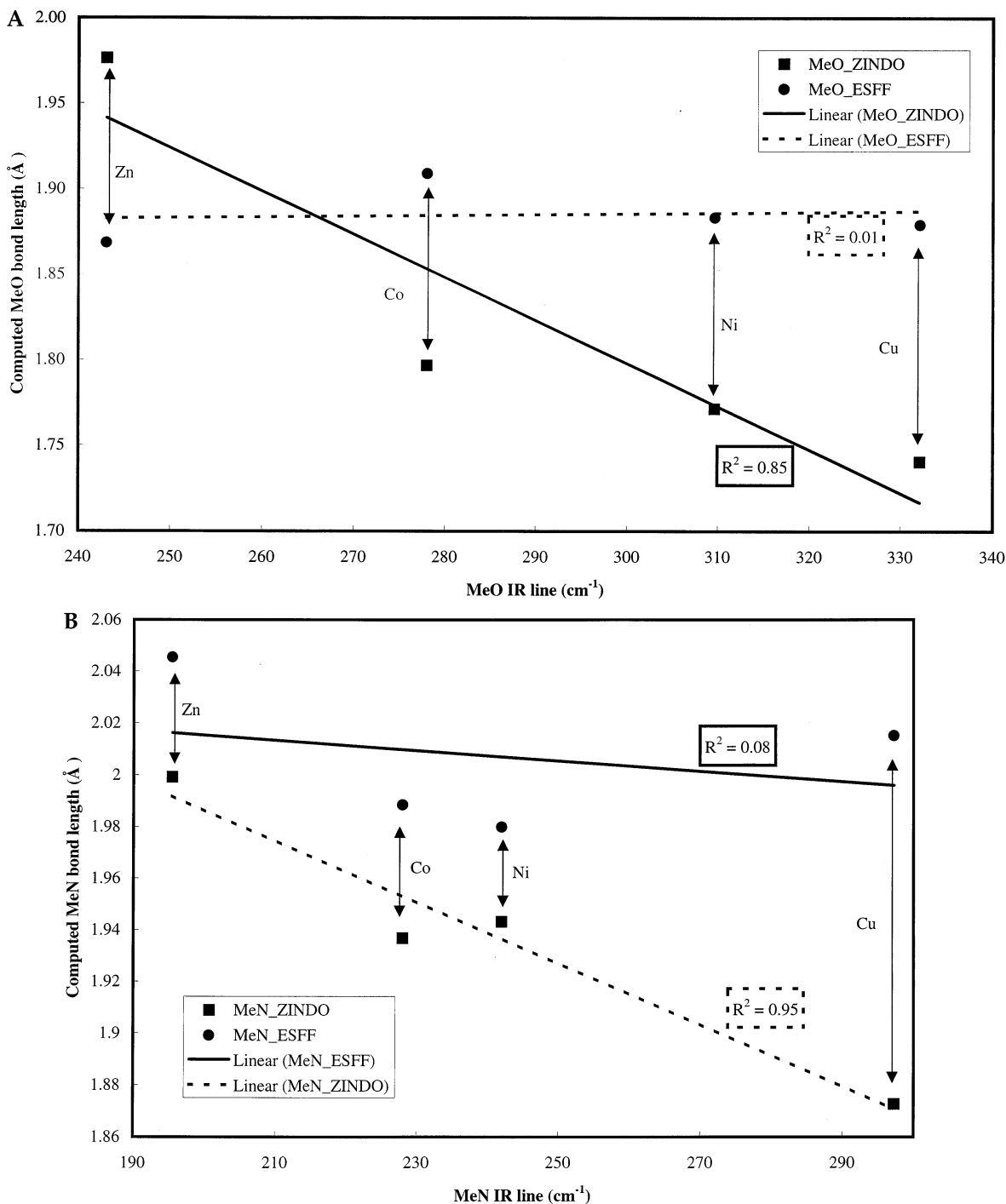


Figure 5. Spectral validation of ZINDO and ESFF calculations. (A) Computed MeO bond length (angstroms) versus MeO IR line; (B) computed MeN bond length (angstroms) versus MeN IR line; (C) computed MeN bond length (angstroms) versus chelate deformation IR line.

time, as well as by the inherent limitations of molecular mechanics. Moreover, these studies do not take into consideration the validation of the calculations over a wider range of metals.

Structural validation based on comparison of bond lengths

The structural validation based on bond lengths is designed to assess the ability of various molecular modelling methods to

predict the structure of complexes over a large range of different elements. To this end, the structural validation based on bond lengths reveals the following:

1. The prediction of MeO bond lengths by ZINDO and ESFF is similar for both monodentate and planar bidentate complexes. As a general rule, the MeO bond lengths are placed in the following order: MeO in Me_xO_y < MeO in monodentate complexes computed with ZINDO < MeO in mo-

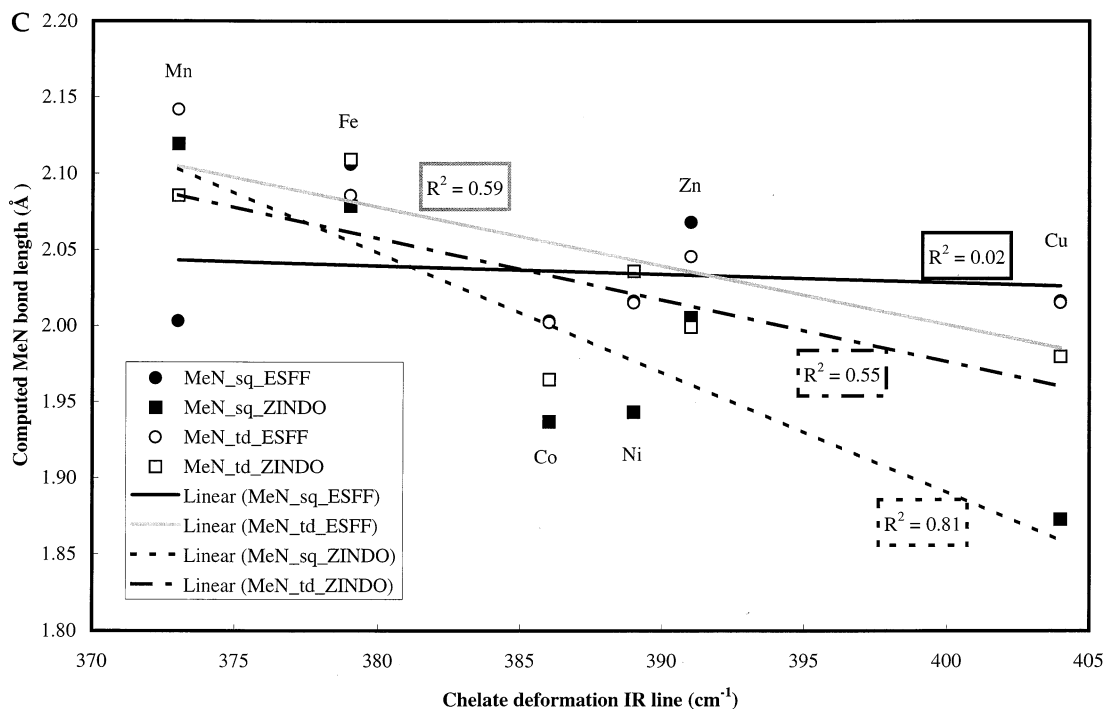


Figure 5. Continued.

nodentate complexes computed with ESFF < MeO in bidentate complexes computed with ZINDO < MeO in monodentate complexes computed with ESFF.

- The computed bond lengths were compared with the corresponding Me_xO_y metal oxides in gas phase.¹⁶ Figure 2A presents the correlation between experimental and computed MeO bond lengths. Apart from the inherent difference between MeO bond lengths in oxides versus predicted values in complexes, ZINDO gives a slightly more consistent trend than ESFF (R^2 of 0.64 versus 0.56, respectively). Both correlations are offset by the presence of anomalous cases (i.e., ruthenium and strontium, for ZINDO and ESFF, respectively).
- ESFF predicts consistently better than ZINDO the MeO bond lengths for planar structures (all X-ray crystallographic coordinates are for this structural type) with an R^2 value of 0.94 versus 0.11, for ESFF and ZINDO, respectively (Figure 2B). The lower correlation for the structures predicted by ZINDO is the result of anomalous values for the titanium complex (if these values are removed, R^2 increases to 0.7) and probably for the zinc complex. The values for the titanium, molybdenum, and silver complexes are for related structures, that is, $\text{Ti}^{4+}(\text{8-hydroxyquinolate})_2\text{Cl}_2$,²¹ $\text{Mo}^{6+}\text{O}_2(\text{8-thio-quinolate})_2$,²² and $\text{Ag}^+(\text{8-hydroxyquinolate})(\text{pyridine})$.²³ The average difference for all data (experimental versus predicted) is 0.1375 and 0.177 Å for ESFF and ZINDO, respectively.
- In contrast to the prediction of MeO bond lengths, ZINDO predicts better the MeN bond length, with correlation coefficients of 0.83 and 0.48 for ZINDO and ESFF, respectively (Figure 2C); the difference lies in the higher MeN values predicted by ESFF as compared with lower values predicted by ZINDO (with the exception of the titanium complex). The average difference for all data (experimental versus predicted) is 0.033 and 0.042 Å for ESFF and ZINDO, respectively.

Structural validation based on overall comparison of structures

The structural validation based on RMS overlay of the computed and experimental or *ab initio* structures is designed to assess the ability of various molecular modelling methods to predict the *overall* structure of the complexes over a narrow range of cases. To this end, the structural validation based on RMS overlay reveals the following:

- The overall prediction of *planar* structures using ZINDO for $\text{Cu}^{2+}(\text{8-hydroxyquinolate})_2$ and $\text{Zn}^{2+}(\text{8-hydroxyquinolate})_2$ structures compared with reported X-ray crystallographic structures (for the copper complex in Figure 3A, for α , β , and γ forms; and for the zinc complex in Figure 3B, for the dihydrate form with water molecules removed) is excellent with overall deviations of 0.035 and 0.018 Å, respectively.
- There is a high degree of similarity between predicted *planar* structures with various methods (ZINDO, ESFF, and DMol) for both copper and zinc complexes (in Figure 3C and D, respectively). The deviations are in the same range as described above.
- A marked difference emerges when comparing *tetrahedral* structures predicted by ZINDO and *ab initio* methods. While the copper complex (Figure 3E) predicted by ESFF is considerably different from the one predicted by both ZINDO and DMol, the prediction of tetrahedral zinc complex (in Figure 3F) is similar for all methods. This can be (partially) explained by the difficulty of both ZINDO and DMol to optimize the nonplanar $\text{Me}^{2+}(\text{8-hydroxyquinolate})_2$ complexes (the calculations had to be stopped before reaching the full optimisation).

The overall conclusion of the structural validation is that ESFF is more robust in terms of structure optimisation, especially for nonplanar structures.

Tendency to form planar versus tetrahedral structures

The comparison of the energies of the planar (square-planar) with nonplanar (tetrahedral) structures shows that ZINDO consistently predicts a tendency of Me^{2+} (8-hydroxyquinolate)₂ to form planar structures, whereas ESFF predicts an overall tendency towards tetrahedral structures (Figure 4). In the case of ZINDO the tendency towards planar structures is to some extent artificially enhanced by the difficulty to reach fully optimised nonplanar structures. Despite this exogenous effect, the prediction of tetrahedral-to-square-planar balance by ZINDO seems more consistent. For instance, ZINDO predicts the increase in the tendency towards planar structures in the first and second row of transition metals (from group VIII to group IB) and then a swing back to tetrahedral structures at the end of the row (for zinc only, as silver and cadmium are not parametrised for ZINDO calculations with spectroscopic γ values). In opposition, ESFF predicts a similar evolution only for the first row of transition metals. Moreover, in absolute terms and with the exception of the silver complex, ESFF does not predict any planar structure as energetically favourable. The multitude of planar or pseudo-planar X-ray crystallographic structures^{18–23} as compared with the scarcity of reported tetrahedral or pseudo-tetrahedral structures (only one structure is reported for zinc,¹⁹ but without crystallographic coordinates) induces the conclusion that ZINDO is in energy terms a better predictor of geometry type (i.e., square-planar versus tetrahedral structure) for Me^{2+} (8-hydroxyquinolate)₂ complexes.

Enthalpy of complex formation versus second ionisation potential

It is reasonable to assume that the higher the second ionisation potential for a bivalent metal ion the higher would be the stability of the complex that reverses this ionisation. This relationship is found to be true for ZINDO calculations but not for ESFF calculations (Color Plate 1). The enthalpy-related energies were in both cases calculated by taking into consideration the energies for the most stable structures.

In the case of ZINDO three classes of relationships seem to emerge from the comparison of SCF energies and the second ionisation potential (data from Ref. 16): (1) the alkaline earth metals (and probably zinc) exhibit a pseudo-linear, independent behaviour (almost the same SCF energy for different second ionisation potentials); (2) the first-row transition metals exhibit a strong correlation between the computed SCF energy of complexes and the second ionisation potential of the respective ions (with a correlation coefficient $R^2 = 0.6$ because of the anomalous data of the zinc complex); and (3) a strong correlation for the second row of transition metals ($R^2 = 0.94$). Apart from the alkaline earth metals (plus zinc) the relationship between SCF energy and second ionisation potential does not follow a linear trend. The strong relationships for transition metals are not only similar in form but to some extent overlap for all data. Moreover, it is interesting to note that the preceding rela-

tionships for ZINDO calculations are valid for both monodentate and bidentate complexes (results not shown) despite the fact that the respective SCF energies are about five times higher for monodentate than for bidentate complexes.

In opposition to ZINDO-predicted relationships, ESFF fails to connect the second ionisation potential with the total potential energy. A similar polynomial fit gives a poor correlation of $R^2 = 0.47$ and 0.5 for the first- and second-row transition metals, respectively.

Enthalpy of complex formation versus standard reduction potential

Using the same line of argument, one would expect to find a similar relationship between the energies associated with the enthalpy of the formation of the complex and the respective standard reduction potential. While ZINDO predicts a strong relationship between SCF energy and the standard reduction potential, ESFF cannot predict any correlation (Color Plate 2). As the standard reduction potential (data from Ref. 16) is a measure of the free enthalpy (including an entropic term) rather than enthalpy, it would be expected that the relationship be more complex than that described above. Indeed, ZINDO calculations now show a clear split between the correlation for the first- and second-row transition metals (with $R^2 = 0.84$ and 0.92 , respectively). Similar to the relationship between the SCF energy and the second ionisation potential, the R^2 values are lower for the first row of transition metals than for the second row, because of anomalous values for zinc. As described above, the relationship for ZINDO calculations is valid for both monodentate and bidentate complexes.

Correlation between predicted bond lengths and experimental spectral data

Because the computation of IR and UV spectra would be beyond the scope of an expeditious, but metal-comprehensive, study, we compared the predicted lengths of the bonds closely involved in the formation of the complexes (i.e., MeO and MeN) with their associated spectroscopic data. Only the bidentate structures were used in the analysis to account for the fact that all spectroscopic data are for bidentate structures.

The comparison of the MeO IR line (data from Ohkaku et al.³⁰) with the MeO bond length in the structures predicted as energetically favourable shows that ZINDO predicts a consistent relationship (Figure 5A) despite the fact that the zinc complex is not in the same structural class with the rest of the data. ESFF fails to predict any relationship despite the fact that all structures are similar (i.e., tetrahedral). The same conclusions can be drawn from a comparison of MeN bond lengths predicted by ZINDO and ESFF with the MeN IR line (data from Ohkaku et al.³⁰), as presented in Figure 5B.

Finally, when comparing the MeN bond lengths in tetrahedral structures with the IR line associated to the deformation of the chelate ring (data from Tackett and Sawyer³¹), ZINDO finds a similar connectivity as ESFF (R^2 of 0.55 and 0.59 , respectively) despite the fact that ZINDO predicts the tetrahedral structural type as energetically unfavourable, in opposition with ESFF prediction. When comparing the MeN bond lengths in square-planar structures (suggested as energetically favourable by the multitude of experimental data) the connectivity predicted by ZINDO is in

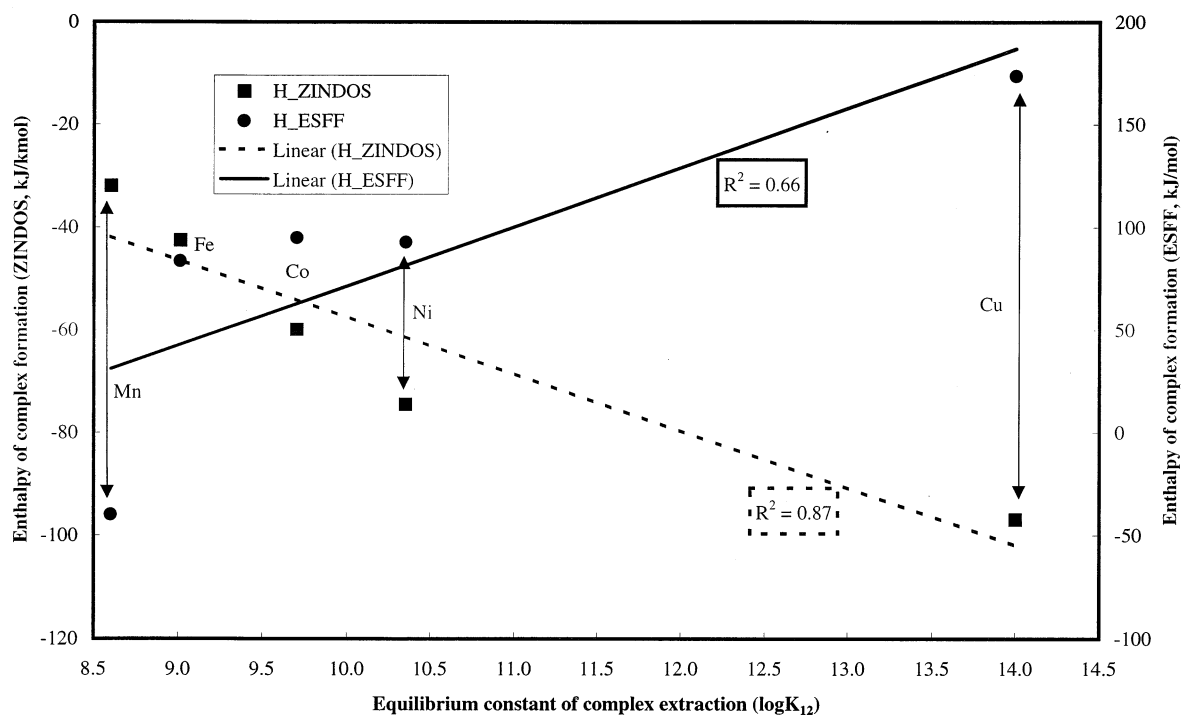


Figure 6. Experimental extraction equilibrium constants ($\log K_{12}$) versus computed "enthalpy of formation" of the complex (monodentate complexes).

striking opposition with the ESFF lack of connectivity (R^2 of 0.81 versus 0.02, for ZINDO and ESFF, respectively).

Correlation between computed energies and experimental equilibrium data

The final step in the assessment of the ability of the ESFF and ZINDO methods to describe the processes associated with the formation of metal complexes attempts to link the molecular modelling data with technologically relevant data. One of the most important technological parameters of the solvent extraction process is the equilibrium constant for the formation and transfer of a complex of a specific ion. The metal-specific equilibrium constant translates into the achievable selectivity versus several ions present in the aqueous phase when using a specific extractant. The computed energies associated with the enthalpy of formation of the complex should, in principle, be connected with the experimental values of the equilibrium constant. It would be expected that the most stable complexes exhibit the highest equilibrium constant (i.e., the equilibrium is tilted towards the presence of the complexes in the organic phase). As the formation of the monodentate complex is the determining step in the overall process of formation of the complexes from the interface between the aqueous phase and the organic phase, as suggested by thorough experimental studies,³² we used in the analysis the energies computed for monodentate complexes (i.e., SCF energy and total potential energy, for ZINDO and ESFF methods, respectively). It was observed, however, that the same conclusions could be drawn from the analysis of the energies calculated for the bidentate complexes.

The comparison of ZINDO- and ESFF-computed energies with experimental extraction constants (data from Stry and Freiser;³³ Figure 6) shows that ZINDO can predict the expected

relationship presented above in a consistent manner ($R^2 = 0.87$). In opposition to the relationship predicted by ZINDO, ESFF suggests an inverse proportionality, albeit with a lower correlation coefficient ($R^2 = 0.66$). The ESFF-predicted relationship suggesting that less thermodynamically favourable complexes will be present in higher concentrations in the organic phase is difficult to substantiate.

Correlation between computed energies and pH of extraction

Another important technological parameter is the $pH_{1/2}$ (i.e., the pH at which the complex is 50% extracted). Because the formation of the complex requires the formation of a chelating bond between the metallic ion and the oxygen atom in 8-hydroxyquinoline, as well as the ionisation of the oxygen atom, it is expected that the pH will be linked to the charge of the oxygen-ligating atom in the $Me^{2+}(8\text{-hydroxyquinolinate})_{1-2}$ complex. Furthermore, it would be expected that the more ionic the character of the MeO bond (i.e., the more electropositive the respective metal) the higher the negative charge at the oxygen atom in the complex. This assumption is validated by ZINDO-predicted charges, but not by ESFF-predicted charges (Figure 7). It follows that higher negative charges at the oxygen atom (required by MeO bonds with higher ionic character) would be obtained at the aqueous/organic interface when a more basic medium is present in the aqueous phase. Finishing this line of argumentation, it might be expected that the complexes that are formed and extracted at a higher pH (according to the data in Stry and Freiser³³) will exhibit higher negative charges at the oxygen-ligating atom. This relationship is consistently predicted by ZINDO ($R^2 = 0.77$), whereas ESFF predicts an opposite relationship (similar

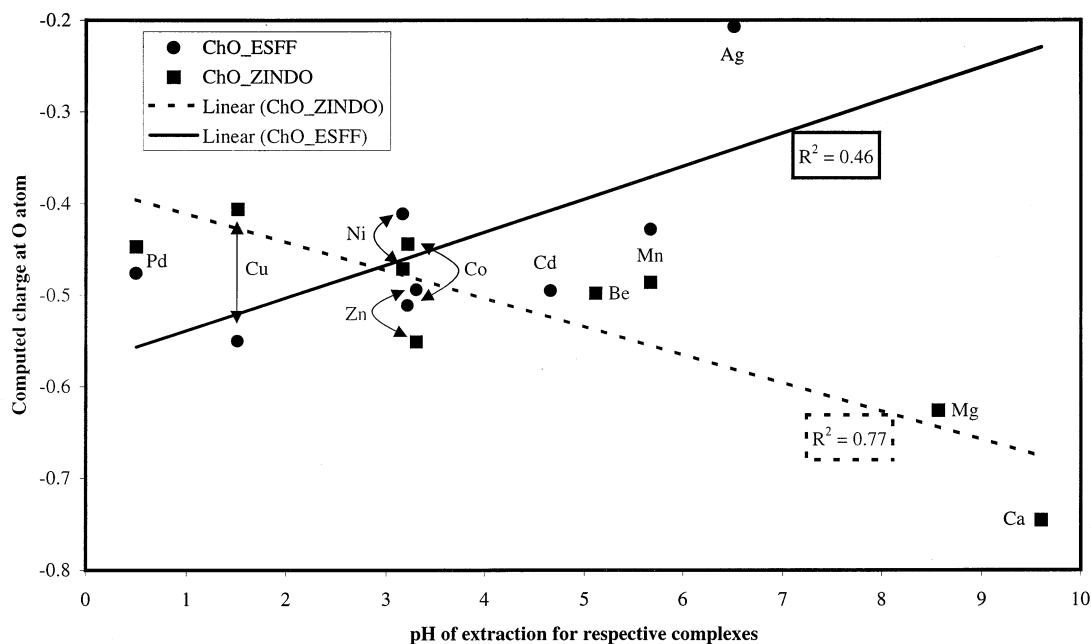


Figure 7. pH of extraction versus computed charge at the ligating oxygen atom (monodentate complexes).

to the case described above), albeit with a lower correlation coefficient ($R^2 = 0.46$).

Comparison of the CPU times required by ZINDO and ESFF methods

To complete the parallel between ZINDO and ESFF one should compare the CPU times required for the optimisation of the system studied, that is, $\text{Me}^{2+}(\text{8-hydroxyquinolate})_{1-2}$ com-

plexes, with ZINDO and ESFF (presented in Figure 8). It is interesting to note that the CPU time required by ZINDO to optimise a complex increases approximately twofold for the complexes containing elements from the first- and second-row transition metals, respectively. However, the relative advantage of ESFF versus ZINDO decreases approximately fourfold from an average ratio of about 40 to one of about 10 when optimising structures containing elements from the first- and second-row transition metals, respectively. Finally, the maximum CPU

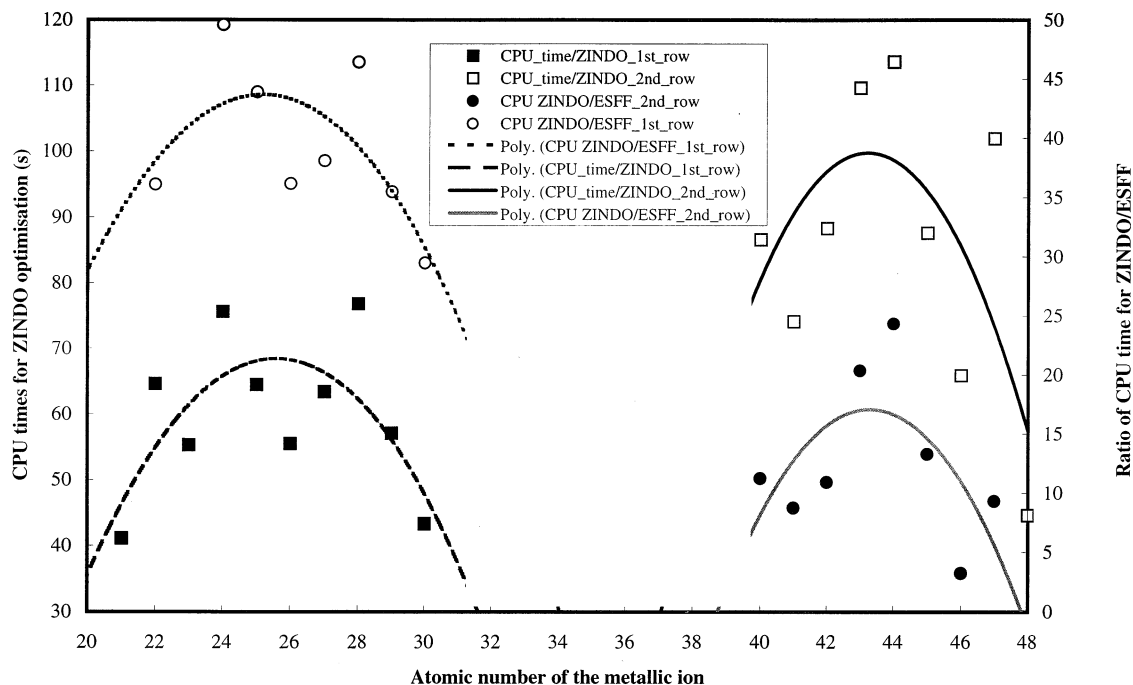


Figure 8. CPU times required for the optimisation of $\text{Me}^{2+}(\text{8-hydroxyquinolate})_{1-2}$ complexes, using ZINDO and ESFF.

times are required for those complexes with elements from the middle transition metal rows.

For the systems studied the CPU times are not considered prohibitive per se, even for ZINDO, but the procedures necessary for finding appropriate nonplanar structures (for ZINDO) and for analysing all alternative structures (for ESFF) contribute importantly to the overall simulation time.

CONCLUSIONS

The $\text{Me}^{2+}(\text{8-hydroxyquinolate})_{1-2}$ system was studied using semi-empirical (ZINDO) and molecular mechanics (ESFF) methods for a range of bivalent metals. The structural validation of the optimisation calculations showed that ESFF is in general an efficient predictor of the structure of the complexes. On the other hand, ZINDO offers an appropriate tool for describing the mechanisms of complex formation for the studied system. For the system studied CPU times are not prohibitive, even for a metal-comprehensive investigation.

ACKNOWLEDGMENTS

The present research was performed while D.V.N. held a Science & Technology Agency of Japan Fellowship and benefited from additional financial support from Rio Tinto, Ltd. The authors thank Geoffrey Stevens for input regarding experimental aspects, Michael Zerner for advice regarding ZINDO, and the technical support staff of Molecular Simulations, Inc., for continuous interaction during the period of this project.

REFERENCES

- 1 Kauffman, G.B. *Inorganic Coordination Compounds*, Heyden & Son, London, 1981
- 2 Allen, F.H., and Kennard, O. 3D Search and research using the Cambridge Structural Database. *Chemical Design Automation News* 1993, 8(1), 1, 31–37
- 3 Anderson, W.A., Edwards, W., and Zerner, M.C. *Inorg. Chem.* 1986, **25**, 2728–2732; Ridley, J.E., and Zerner, M.C. *Theor. Chim. Acta* 1976, **42**, 223; other references regarding ZINDO: Ridley, J.E., and Zerner, M.C. *Theor. Chim. Acta*, 1973, **32**, 111; Bacon, A.D., and Zerner, M.C. *Theor. Chim. Acta*, 1979, **53**, 21; Zerner, M.C., Loew, G.H., Kirchner, R., and Mueller-Westerhoff, U. *J. Am. Chem. Soc.*, 1980, **102**, 589; Head, J.D., and Zerner, M.C. *Chem. Phys. Lett.*, 1985, **122**, 264; Head, J.D., and Zerner, M.C. *Chem. Phys. Lett.*, 1986, **131**, 359; Edwards, W.D., and Zerner, M.C. *Theor. Chim. Acta* 1987, **72**, 347
- 4 Shi, S., Yan, L., Yang, Y., and Shaulsky, J. ESFF Force Field Project Report. Molecular Simulations, Inc., San Diego, California, 1994
- 5 Veillard, A., Ab initio calculations of transition-metal organometallics: Structure and molecular properties. *Chem. Rev.* 1991, 91, 743–766
- 6 Yu, J., and Hehre, W.J. To be published (1998)
- 7 Comba, P., and Hambley, T.W. MOMECC, a molecular mechanics package for transition metal complexes, 1995; Bernhardt, P.V., and Comba, P. *Inorg. Chem.* 1992, **31**, 2638
- 8 Stry, J. *The Solvent Extraction of Metal Chelates*. Butterworths, London, 1965
- 9 Ritcey, G.M., and Ashbrook, A.W. *Process Metallurgy*, Part II: Solvent Extraction: Principles and Application to Process Metallurgy. Elsevier, Amsterdam, 1979
- 10 Sahni, S.K., and Reedijk, J. Coordination chemistry of chelating resins and ion exchangers. *Coord. Chem. Rev.* 1984, 59, 1
- 11 Cullogh, J.K., Fornasiero, D., Perera, J.M., Stevens, G.W., and Grieser, F. An NMR Study of the Adsorption of a Metal Chelating Agent at a Micelle/Water Interface. *J. Coll. Int. Sci.*, 1993, (157), 180; Sperline, R.P.; Freiser, H. Adsorption at the Liquid-Liquid Interface Analyzed by in Situ Infrared Attenuated Total Reflection Spectroscopy, *Langmuir*, 1989, **6**, 344–346; Tondre, C. & Hebrant, M. Kinetics of Extraction of Copper(II) by Micelle Solubilized Complexing Agents of Varying Hydrophilic Lipophilic Balance. 2. Interfacial Versus Bulk Aqueous-Phase Mechanisms. *J. Phys. Chem.* 1992, **96**, 11079–11085
- 12 Molecular Simulations, Inc. InsightII User's Manual; Discover3 User's Manual. Molecular Simulations Inc., San Diego, California, 1996
- 13 Zerner, M.C. ZINDO: A Semi-Empirical Program Package. University of Florida, Gainesville, Florida, 1996
- 14 Molecular Simulations, Inc. InsightII User's Manual; ZINDO User's Manual. Molecular Simulations, Inc., San Diego, California, 1996
- 15 Molecular Simulations, Inc. DMol 96.0/4.0.0 Quantum Chemistry User's Guide. Molecular Simulations, Inc., San Diego, California, 1996
- 16 Lide, D.R. (ed.) *CRC Handbook of Chemistry and Physics*, 73rd Ed. CRC Press, Boca Raton, Florida, 1992
- 17 Cambridge Crystallographic Database Centre. Cambridge Crystallographic Database System, CCDS. Cambridge Crystallographic Database Centre, Cambridge, 1996. [And references therein]
- 18 For the copper complex: Merrit, L.L., Jr. X-ray structure determinations: Some compounds of interest in analytical chemistry. *Anal. Chem.* 1953, **5**, 25, 718–721; Hoy, R.C., and Morris, R.H. The crystal structure of the α form of anhydrous copper 8-hydroxyquinolate. *Acta Crystallogr.* 1967 **22**, 476–482; Palenik, B.J. The structure of coordination compounds. II. The crystal and molecular structure of the beta form of anhydrous copper 8-hydroxyquinolate. *Acta Crystallogr.* 1964, **17**, 687–695; Kanamaru, F., Ogawa, K., and Nitta, I. *Bull. Chem. Soc. Jpn.* 1963, **36**, 422; Ammor, S., Coquerel, G., Perez, G., and Robert, F. *Eur. J. Solid State Inorg. Chem.* 1992, **29**, 445
- 19 For the zinc complex: Merrit, L.L., Caddy, R.T., and Mundy, B.W. The crystal structure of zinc 8-hydroxyquinolate dihydrate. *Acta Crystallogr.* 1954, **7**, 473–476
- 20 For the palladium complex: Prout, C.K., and Wheeler A.G. *J. Chem. Soc. A* 1966, **62**, 1286
- 21 For the titanium complex: Studd, B.F., and Swallow A.G. *J. Chem. Soc. A* 1968, **64**, 1961
- 22 For the molybdenum complex: Yamanouchi, K., and Enemark J.H. *Inorg. Chem.* 1979, **18**, 1626
- 23 For the silver complex: Fleming, J.E., and Lynton, H. *Can. J. Chem.* 1968, **46**, 471
- 24 Guesnet, P., Sabot, J.L., and Bauer, D. Kinetics of cobalt oxidation in solvent extraction by 8-quinolinol and Kelex-100. *J. Inorg. Nucl. Chem.* 1980, **42**, 1459–1469
- 25 Cai, R., Freiser, H., and Muralidharan, S. Kinetics of the dissociation of nickel-2-methyl-8-hydroxyquinoline, in

- water and surfactant micelles. *Langmuir* 1995, 11, 2926–2930
- 26 Boumezioud, M., Tondre, C., and Lagrange, P. Effect of an alkyl chain substituent on the kinetics and thermodynamics of complexation of 8-hydroxyquinoline with Ni^{2+} and Co^{2+} in methanolic solutions. *Polyhedron* 1988, 7, 513–521
 - 27 Gatrone, R.C., and Horwitz, E.P. Molecular modelling of organic extractants. *Solv. Extr. Ion Exch.* 1988, 6, 937–972
 - 28 Sella, C., and Bauer, D. A molecular modeling study of zinc(II) extraction by substituted 8-hydroxyquinolines in the presence of various pyridinic adducts. *Sep. Sci. Tech.* 1993, 28, 2137–2148
 - 29 Stephan, H., Gloe, K., Kruger, T., Chartroux, C., Neuman, R., Weber, E., Mockel, A., Woller, N., Subkew, G., and Schwuger, M.J. Extraction behaviour and molecular modelling of position isomers of alkyl-8-hydroxyquinoline derivatives. *Solv. Extr. Res. Dev. Jpn.* 1996, 3, 43–55
 - 30 Ohkaku, N., and Nakamoto, K. Metal isotope effect on metal–ligand vibrations. Metal complexes of 8-hydroxyquinoline. *Inorg. Chem.* 1970, 10, 798–805
 - 31 Tackett, J.E., and Sawyer, D.T. Properties and infrared spectra in the potassium bromide region of 8-quinolinol and its metal chelates. *Inorg. Chem.* 1963, 3(5), 692–696
 - 32 Dietz, M.L., and Freiser, H. Role of the interface in kinetics and mechanisms of nickel extraction with certain halogen- and alkyl-substituted 8-quinolinols. *Langmuir* 1991, 7, 284–288
 - 33 Stary, J., and Freiser, H. Equilibrium Constants of Liquid–Liquid Distribution Reactions, *Part IV: Chelating Extractants*. Pergamon Press, Oxford, 1975